

DEVELOPMENT OF MgO CERAMIC STANDARDS FOR X-RAY AND NEUTRON LINE BROADENING ASSESSMENTS

Suminar Pratapa[§] and Brian O'Connor
Materials Research Group, Department of Applied Physics
Curtin University of Technology, Perth, WA 6845 Australia

ABSTRACT

An MgO ceramic line profile standard has been developed for strain-size evaluations with x-ray diffraction (XRD) and neutron diffraction (ND) data. The production of these is of interest to the authors for general-purpose XRD and ND line profile work as the popular LaB_6 NIST SRM 660 standard cannot be used in neutron investigations due the severity of neutron attenuation. The basis of developing the MgO standard was achieving strain relief through sintering at a designated temperature and slow annealing during cooling. A series of MgO sintering trials was conducted to establish the relationship between line profile shape and sintering conditions. An MgO ceramic sintered at 1450°C for 2 hours displayed comparable Bragg-Brentano XRD broadening with that of the LaB_6 NIST standard. The XRD Williamson-Hall plots for both materials showed negative slopes indicating that both have minimal strain. Crystallite size broadening is also minimal for the MgO and LaB_6 standards, according to XRD Rietveld analyses and electron microscopy imaging. These results confirm that the MgO ceramic is suitable for line broadening corrections with both XRD and ND data.

INTRODUCTION

In powder diffraction strain-size analysis, there is a requirement to know the shape of the instrument line profile (*g*) which originates from the non-ideal optical effects of the diffractometer and the wavelength distribution of the radiation. A diffraction profile measured with a structurally imperfect material (*h* profile) is a convolution of the profile *f* due to crystallite imperfections (non-uniform microstrain, small crystallite size, stacking faults) and the *g* profile [1]. There are two general strategies for obtaining the specimen profile *f* using the instrument profile *g*:

1. deconvolution of *g* from the measured profile *h*;
2. convolution of *g* with calculated *f* to obtain a calculated line profile which is then compared with the measured profile *h*.

Although simulation of the *g* profile is possible (e.g. [2,3]), some of the instrument characteristics cannot be determined directly with sufficient accuracy [4]. Therefore, measuring *g* for correction of the instrument profile is more precise and reliable, provided that a suitable standard specimen is available.

A standard specimen for instrument correction should meet the following conditions [4,5]:

a. does not exhibit measurable specimen broadening;
b. (ideally) is developed from the same material as the specimen to be investigated;

[§] Currently on leave from Department of Physics, Institute of Technology 10 November Surabaya (ITS), Indonesia.

c. should not exhibit pronounced transparency;
d. exhibits minimal statistical errors associated with excessively large crystallites.

The development of an acceptable standard from the same material as the test specimen for strain-size evaluations is rarely achievable due to difficulties with specimen preparation [4]. Therefore, much effort has been directed towards developing instrument broadening standards for general use, notably the LaB_6 NIST SRM 660 powder for x-ray diffraction [6]. This paper reports the development of a standard specimen for instrument broadening corrections by sintering of MgO powder at 1450°C for 2 hours and subsequent annealing. The suitability of the MgO standard was assessed by comparing the line broadening characteristics and the microstructure with those for LaB_6 NIST SRM 660.

The MgO ceramic standard is particularly useful for single-line strain-size evaluation of MgO ceramics since no Bragg peak position correction required. Moreover, the standard is applicable not only for x-ray diffraction data but also for neutron diffraction data where LaB_6 cannot be used due to severe neutron attenuation.

EXPERIMENTAL PROCEDURE

A suite of MgO ceramic materials was prepared from an MgO powder of specified purity 99% (Aldrich Chemicals, USA), containing approximately 10% of $Mg(OH)_2$. The MgO powder was calcined at 1100°C for 60 minutes to convert the hydroxide to oxide. The calcined powder was uniaxially pressed at ≈ 38 MPa in a metal die to form a set of cylindrical specimens of diameter 19 mm. The pressed MgO powders were then sintered at designated temperatures - 1100°C for 2 hours, 1250°C for 2 hours, 1450°C for 2 hours and 1600°C for 6 hours - to give systematic variations in broadening effects. A slow annealing of 2°C per minute was selected to avoid the development of the thermal residual strains during cooling.

A Siemens D500 Bragg-Brentano diffractometer, with a Cu tube ($\lambda_{K\alpha 1}$ = 1.54056 Å) operating at 40 kV and 30 mA, with an incident beam divergence slit = 0.3°, receiving slit = 0.15°, post-diffraction graphite analyser, and NaI detector with pulse discrimination, was used to collect x-ray data. Samples were rotated during data collection to improve the crystal statistics [4]. Sets of reflections were selected for the LaB_6 SRM and the MgO specimens for peak profile analysis. The peak intensity of each reflection was at least 4,000 counts. These data were measured with step-size = 0.02° and counting time per step = 2 - 40 s. Whole-pattern data were also measured for both samples for Rietveld analysis using step-size = 0.02°, counting time per step = 1 s and 2θ range = 10-150°.

Neutron diffraction data were acquired with the fixed-wavelength, high-resolution powder diffractometer at the Australian Nuclear Science and Technology Organisation's research reactor HIFAR at Lucas Heights, Australia [7]. The instrument is configured with 24 He^3 detectors. Specimens approximately 15 mm diameter and 50 mm high were positioned on a rotating table. The conditions of measurement were step-size = 0.05°, 2θ range = 5-150°, counting time per step ≈ 13s and wavelength 1.493Å. Corrections for incident beam fluctuations were made using an incident-beam monitor.

Peak profile analysis was performed using the *SHADOW* program (*Release 4.2*, Materials Data Inc., 1999), with the pseudo-Voigt and Voigt functions being selected to fit the peak shape. The

full-width at half-maxima (FWHM) obtained from fitting with the pseudo-Voigt function were plotted against 2θ. The Voigt function, which is the convolution of the Gaussian with the Lorentzian functions, was used to extract the strain-size estimates following the single-line method described by Keijser *et al.* [8]. In this method, strain is assumed to contribute only to the Gaussian component; while size contributes only to the Lorentzian component.

Rietveld refinements were performed with the program *Rietica* [9]. The Gaussian component of the FWHM, H_G, is described by the Caglioti expression [10]

$$H_G^2 = U \tan^2 \theta + V \tan \theta + W \qquad (5)$$

where U, V, and W are refineable parameters. The Lorentzian component (H_L) is described by the Scherrer equation

$$H_L = \frac{\lambda}{D} \sec \theta \qquad (6)$$

with D being the crystallite dimension along the scattering vector and λ the wavelength.

The refinements involved adjustment of U and D, the lattice parameters, the phase scale factors, the background polynomial parameters, the 2θ-scale offset and the asymmetry parameters. The V and W parameters were fixed to the values obtained with the LaB_6 standard by assuming that strain contributes only to the U parameter. The expression for calculating root-mean-square strains can be found elsewhere [11]. The preferred-orientation parameter was not refined. Crystal data for MgO and LaB_6 were taken from the Inorganic Crystal Structure Database (FachInformationsZentrum and Gmelin Institute, Germany) - ICSD Collection Code 9863 - referring to Sasaki *et al.* [12] and ICSD Collection Code 30891 - referring to Korsukova *et al.* [13], respectively.

RESULTS AND DISCUSSION

Figure 1 shows the XRD and ND FWHM *versus* 2θ for MgO ceramic specimens sintered at 1100-2h, 1250-2h, 1450-2h and 1600-6h. It is clear that the sintering causes progressive reduction in XRD and ND FWHMs until 1450-2h, after which there is an increase in the FWHM when more prolonged sintering is applied. The XRD FWHM for the 1600°C ceramic is substantially higher than that for the 1450°C ceramic over the 2θ range, whereas the corresponding FWHMs are very similar for the ND data. These XRD and ND FWHM plot behaviours indicate that there is minimal broadening for both the near-surface and the bulk, respectively.

Figure 2 shows that the XRD FWHM for the MgO ceramic sintered at 1450°C for 2 hours is marginally lower than that for the LaB_6 SRM. Also shown is a comparison of the ND FWHM data with values for the NIST α-Al_2O_3 powder (NIST SRM 676). The MgO ND widths are slightly less than the α-Al_2O_3 widths.

The Williamson-Hall plots (Figure 3) show that the slope of the line for the MgO 1450-2h ceramic is negative, as also found for the LaB_6 SRM. This negative slope indicates that strain broadening must be very small [14].

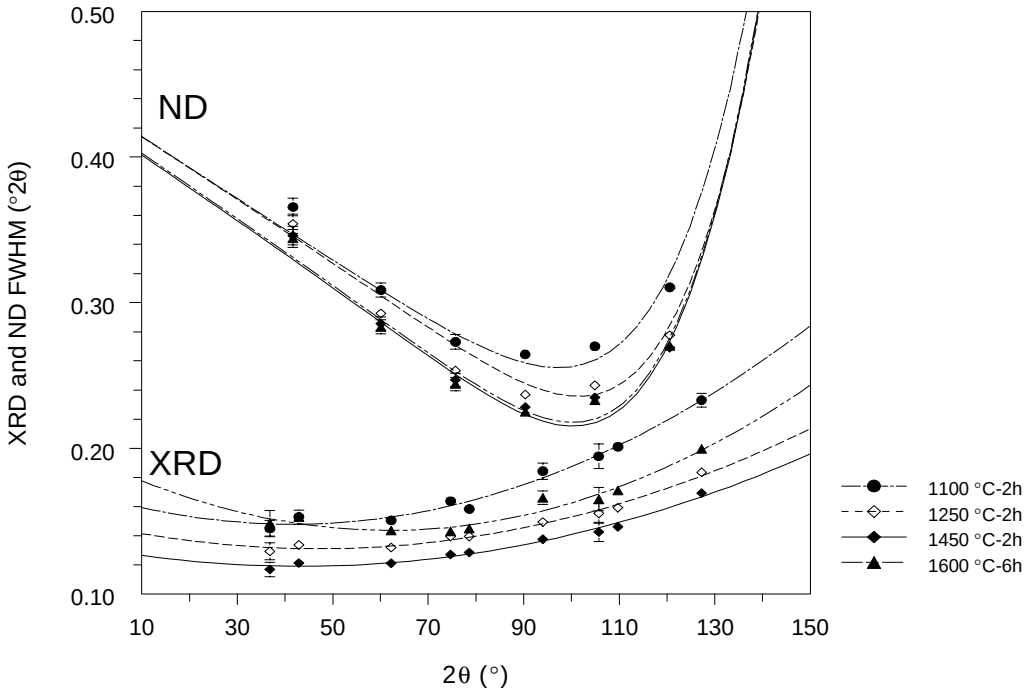

Figure 1. The XRD and ND FWHM versus *2θ* for the MgO ceramics according to sintering conditions. The 1450°C-2h ceramic shows the least broadening. Error bars indicate 1× standard deviation.

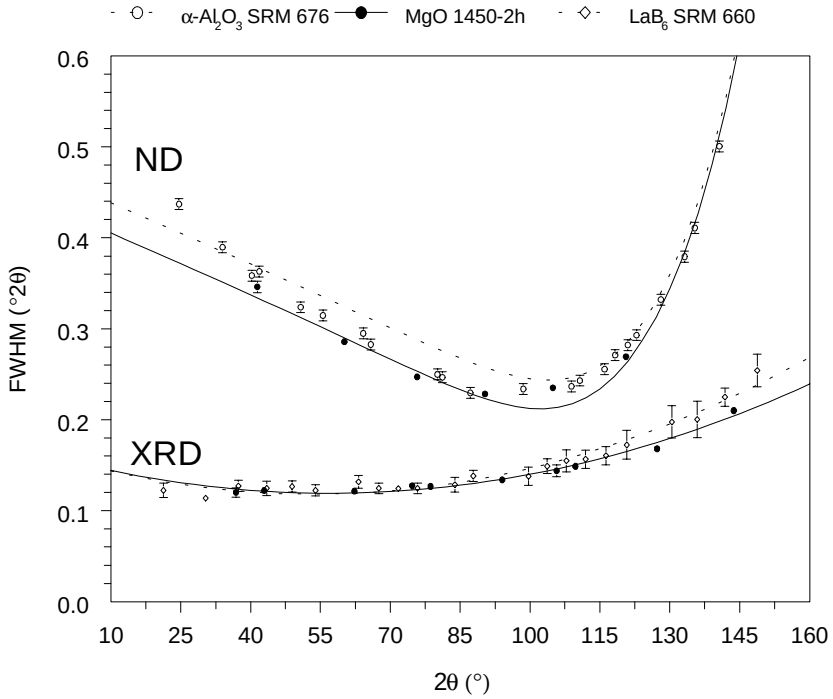

Figure 2. The XRD and ND FWHM versus *2θ* for the MgO ceramic standard (1450°C-2h) compared with the LaB_6 and α-Al_2O_3 NIST SRMs. Error bars indicate 1× standard deviation.

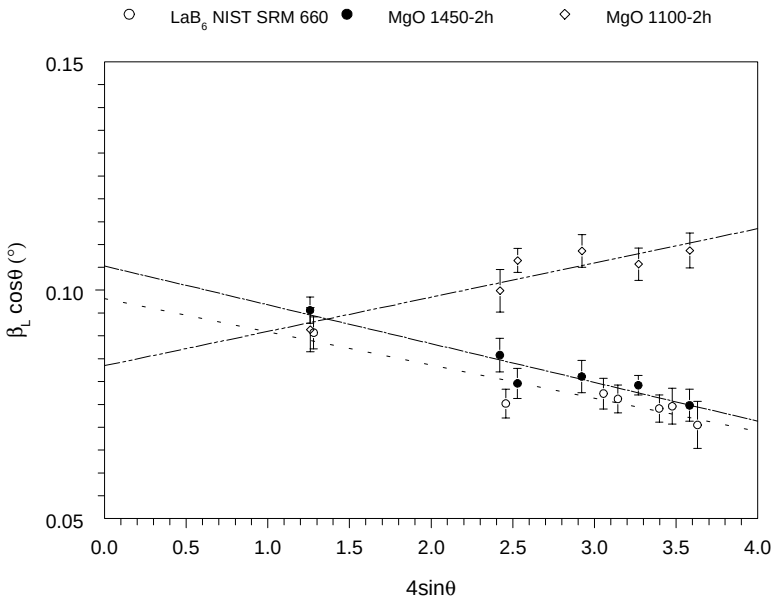

Figure 3. Williamson-Hall plots for the MgO 1450-2h ceramic and the LaB_6 SRM. The 1450-2h ceramic shows similar broadening to that for the LaB_6 SRM. The plot for the strained MgO 1100-2h ceramic is also presented for comparison. Error bars indicate 1× standard deviation.

Figure 4 displays the SEM micrographs of the MgO 1450-2h ceramic and LaB_6 SRM. For both materials, the grain size ranges between approximately 5 and 10 μm. The MgO grains tend to form regular, semi-spherical shapes. With these microstructural characteristics, the ceramic can be expected to give low errors due to crystal statistics [4]. Also, crystallites within this size range give no broadening [4].

From these results it can be inferred that strain/size broadening is negligible and that the MgO 1450-2h ceramic is suitable for instrument profile corrections. In contrast with this result, the positive slope for the MgO 1100-2h ceramic (Figure 3) indicates the presence of strain.

Table 1 depicts the XRD FWHMs for the MgO standard ceramic (200, 311 and 422 reflections) and the LaB_6 SRM (111, 311, 332, 422 reflections). The reflections were selected to represent the low, medium and high angle regions, respectively. The Rietveld Gaussian and Lorentzian FWHMs for the standards are also presented in the table. It is clear that the MgO ceramic has comparable broadening with the LaB_6 SRM. These results support the observation that the broadening characteristics of the ceramic are very similar to the LaB_6 SRM.

The ceramic standard has been used to evaluate strain and size in MgO ceramics using XRD and ND data. The evaluation was performed by the single-line method [8]. Figure 5a shows the XRD and ND strain values for the MgO ceramics as a function of sintering temperature. It is obvious that sintering up to 1450°C for 2 hours causes strain-relief and further sintering generates additional strain. It is likely that the intragranular shear interactions during prolonged sintering increase strain. Sintering also favours crystallite growth in the pure MgO specimens (Figure 5b). For example, from the ND data, the crystallite size increases from 60(1) nm (powder) to 102(3) nm (1100°C-2h) and then to 245(33) nm (1250°C-2h). Detail of the strain-size evaluation are given elsewhere [11].

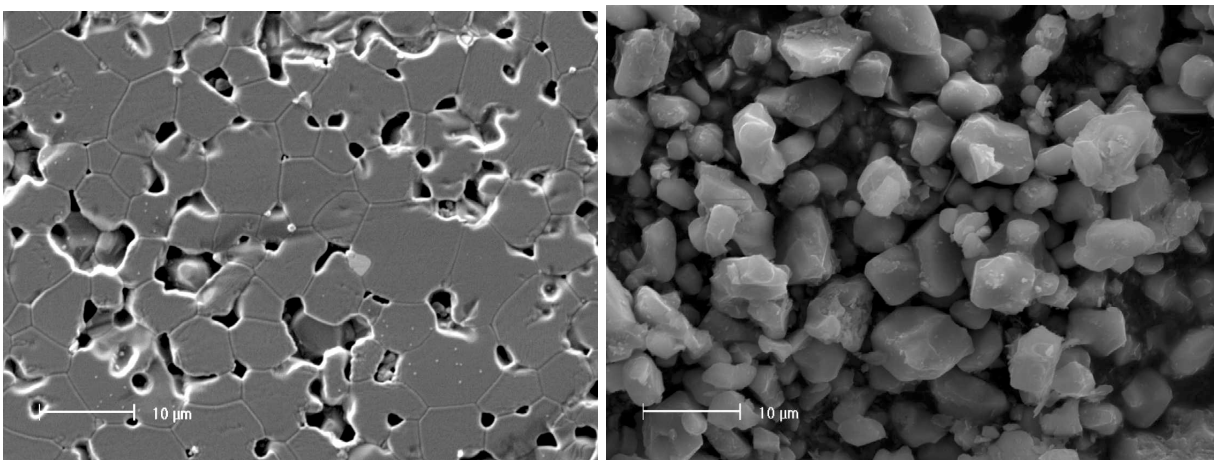

Figure 4. Scanning electron micrographs of the MgO 1450°C-2h standard ceramic (left) and LaB_6 NIST SRM 660 powder (right). Note that the grain size of both materials ranges from 5-10 µm.

Table 1. XRD single-line and Rietveld FWHMs for the MgO standard and the LaB_6 NIST SRM. Estimated standard deviations for the least significant digit are given in parentheses.

				Rietveld	
	hkl	2θ (°)	FWHM (°)	Gaussian (°)	Lorentzian (°)
MgO	111	36.68	0.128(3)	0.0001(1)	0.0309(3)
	311	74.47	0.131(3)		
	422	127.15	0.171(4)		
LaB_6	111	37.28	0.126(4)	0.0007(3)	0.0320(6)
	311	75.67	0.131(5)		
	332	120.64	0.168(7)		
	422	130.39	0.188(7)		

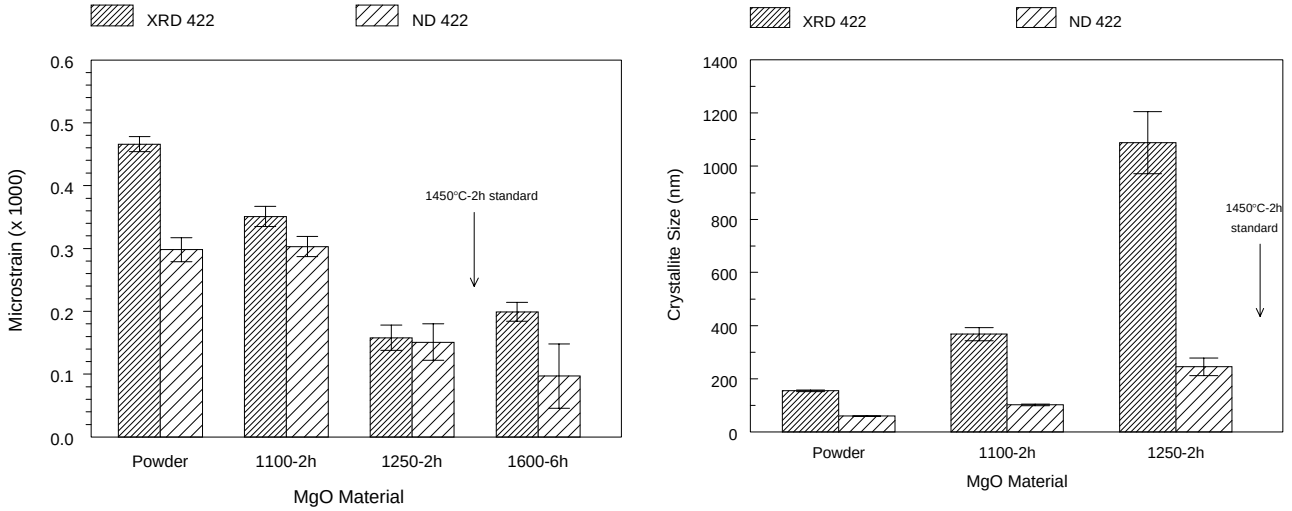

Figure 5. Single-line strain and size estimates for the MgO ceramics determined with XRD and ND data. The MgO 1450°C-2h ceramic was used as the standard for the instrument broadening corrections. Error bars indicate 1× standard deviation.

CONCLUSIONS

It was concluded from the study that:-

1. An MgO ceramic sintered at 1450°C for 2 hours and slow annealing during cooling is suitable for instrument profile corrections using both XRD and ND data. The XRD strain broadening and the microstructural characteristics of the ceramic are very similar to those for the LaB_6 NIST SRM 660.
2. The use of the MgO ceramic standard can be extended to ND for which LaB_6 cannot be used due to severe neutron absorption.
3. The MgO ceramic standard has been used successfullt to evaluate strain-size in MgO ceramics.

ACKNOWLEDGEMENTS

We wish to acknowledge the Australian Agency for International Development (AusAID) for providing a PhD scholarship to S.P., the Australian Institute of Nuclear Science and Engineering (AINSE) - grant numbers 00/119P and 01/112 - for funding the ND data measurements, and Dr Brett Hunter of the Australian Nuclear Science and Technology Organisation (ANSTO) for his assistance and advice with the ND data collection.

S.P. is grateful to the Australian Agency for International Development (AusAID) for awarding a PhD scholarship.

REFERENCES

[1] Klug, H.P. and Alexander, L.E. (1974). *X-ray diffraction procedures for polycrystalline and amorphous materials*. 2nd ed. New York: John Wiley.
[2] Timmers, J., Delhez, R., Tuinstra, F. and Peerdeman, F. (1992). *Accuracy in Powder Diffraction II*, NIST Special Publication 846, edited by E. Prince and J.K. Stalick (U.S. Government Printing Office, Washington), 217.
[3] Cheary, R.W. and Coelho, A.A. (1998). *J. Appl. Cryst.*, **31**, 851-861.
[4] Van Berkum, J.G.M., Sprong, G.J.M., De Keijser, Th.H. and Delhez, R. (1995). *Powder Diffraction*, **10**(2), 129-139.
[5] Leoni, M., Scardi, P. and Langford, J.I. (1998). *Powder Diffraction*, **13**(4), 210-215.
[6] Rasberry, S.D. (1989). *Certificate of Analysis, Standard Reference Material 660. Instrument Line Position and Profile Shape Standard for X-ray Powder Diffraction*. National Institute of Standards and Technology, Gaithersburg, MD.
[7] Howard, C.J., Ball, C.J., Davis, R.L. and Elcombe, M.M. (1983). *Aust. J. Phys.* **36**, 507-518.
[8] Keijser, Th. H. de, Langford, J.I., Mittemeijer, E.J. and Vogels, A.B.P. (1982). *J. Appl. Cryst.* **15**, 308-314.
[9] Hunter, B.A. (1998). *International Union of Crystallography, Commission on Powder Diffraction - Newsletter* **20**, 21.
[10] Caglioti, G., Paoletti, A. and Ricci, F.P. (1958). *Nucl. Instrum.* **3**, 223-228.
[11] Pratapa, S., O'Connor, B. and Hunter, B. (2001). Submitted to *J. Appl. Cryst*.
[12] Sasaki, S., Fujino, K. and Takeuchi Y. (1979). *Proc. of the Japan Academy* **55**, 43-48.
[13] Korsukova, M.M., Lundstroem, T., Gurin, V.N. and Tergenis, L.-E. (1984). *Zeit. f. Krist.*, **168**, 299-306.
[14] Langford, J.I., Cernik, R.J. and Louer, D. (1991). *J. Appl. Cryst.*, **24**, 913-919.